2020-05-17

Optimization of Catalytic Microreactors for Ammonia Decomposition

Eva R. Bove
Worcester Polytechnic Institute

Victoria Cunningham
Worcester Polytechnic Institute

Optimization of Catalytic Microreactors for Ammonia Decomposition

A Major Qualifying Project Report:

Submitted to the Faculty of

WORCESTER POLYTECHNIC INSTITUTE

in partial fulfillment of the requirements for the

Degree of Bachelor of Science

in

Chemical Engineering

by

Victoria Cunningham

Eva Bove

Date: May 18th, 2020

Abstract

Hydrogen is an attractive source for zero-emission energy because of its usefulness in fuel cell batteries. However, traditional methods to capture hydrogen for use in these cells, such as steam reforming, produce greenhouse gases. Ammonia decomposition is a promising method to produce hydrogen, and our research explored the possibility of using catalyst-coated microreactors to improve the decomposition reaction. Microreactors have unique benefits over traditional reactors such as their mass and heat transport properties, precision controls, and improved safety. In our project, we created stainless steel tubular microreactors that are wall-coated with a nickel alumina catalyst. In lieu of testing the physical reactors because of laboratory constraints, we varied parameters of the microreactors by modeling heat transfer properties.

Acknowledgements

We would like to extend our thanks to the following people and departments:

Our advisor Professor Andrew Teixeira for his constant guidance and support throughout the entire project.

Cameron Armstrong for demonstrating lab techniques and offering advice for our project.

Tom Partington for his assistance in the machine shop and Doug White for his help with the XRD data.

The Mechanical Engineering department for assistance with the optical profilometer.

And finally, we would like to thank the Chemical Engineering Department for helping us develop the skills throughout our four years at WPI that made our senior project possible.

Table of Contents

Table of Figures

Section 1: Introduction

1.1 Ammonia Decomposition for Hydrogen Production

Hydrogen is an attractive source for zero-emission energy because of its usefulness in fuel cell batteries. Those fuel cells have potential to power transportation, consumer goods, and even entire grids, if utilized correctly. However, the current methods for producing hydrogen create a number of undesirable byproducts. The most common hydrogen production method is steam reformation, which produces CO_2 and CO. Other methods for production of hydrogen, such as the electrolysis of water, do not produce unwanted products, but can be costly and have low efficiency (Dincer & Acar, 2014). Once the hydrogen is produced, it can pose a challenge to store, as hydrogen requires specialized storage equipment and transportation, which can increase costs and expend more energy (Dincer & Acar, 2015).

Ammonia decomposition is a promising method to produce hydrogen for fuel cells. During the ammonia decomposition process, ammonia is broken down to produce gaseous hydrogen and nitrogen. Unlike methane capture, the products of ammonia decomposition do not inhibit hydrogen production; CO_2 and CO byproducts during methane capture inhibit steam reformation (Adiya et al., 2017). Additionally, ammonia has a higher energy density and is easier to transport, which would allow for possible on-site production of hydrogen for fuel cells.

Ammonia is one of the most significant chemicals for worldwide use—especially in nitrogen-based fertilizers, which are necessary for food production. The ammonia synthesis process was scaled up to an industrial size by Fritz Haber and Carl Bosch (ergo the Haber-Bosch process) in the early twentieth century but requires high temperatures and pressures, usually 400 to 500°C and 150 to 400 atm respectively, due to the reluctance of nitrogen gas to react. Although the Haber-Bosch process remains relatively unchanged over 100 years later, more than 175 million

metric tons are produced per year (Pattabathula & Richardson, 2016). This ammonia could be decomposed into hydrogen for the fuel cells, however traditional ammonia decomposition equipment and plants can be large and bulky. A more energy-efficient approach to ammonia decomposition is utilizing microreactors with wall-coated catalysts, as opposed to a packed-bed reactor in which a gas flows over a solid catalyst. In this project, we explore the potential of manufacturing wall-coated microreactors to increase the energy efficiency of ammonia decomposition.

1.2 Microreactors in Industry

Microreactors are generally considered to be a reactor that has a channel length of less than 1 millimeter. While microreactors can be a variety of geometries, most microreactors are typically a series of small channels or tubes. Currently, microreactors are predominantly used in analytical equipment and in small-scale synthesis of products. Unfortunately, they are not yet widely used in production or synthesis capacity, which can be attributed to the difficulty of scaling up laboratory results into effective processes (Watts & Wiles, 2007). Other sources suggest that patents on microreactors prevented widespread investigation and implementation, but recent expiration of these patents could be part of the resurgence of the microreactor (Tanimu et al., 2017). Cost remains a largely prohibitive factor, as microreactors are newer in the field and require significant advantages to be implemented (Roberge et al., 2008). Scaled up production can be a barrier to implementation of microreactors, and reliable production methods are needed (Kockmann & Roberge, 2011).

1.2.1 Analytic Equipment

In addition to synthesis of products, microreactors are often used for analytics for various reactions and processes. According to Haswell and Watts, microreactor research has mainly

focused on creating Miniaturised Total Analytic Systems, which would allow for localized sample testing (2003). Microfluidics can be studied through microreactors, which can explore the reaction kinetics of a particular process (Mozharov et al., 2011). The fluid flow and reactor conditions can be precisely controlled, which allows for better analysis of reaction kinetics. Gas chromatography is one of the most prominent analytical techniques that uses microreactors, as the process requires the gaseous components to interact with catalyst-coated reactor walls (Li & Liu, 2019). Gas chromatography analyzes small amounts of gas and is the only technique that allows for specific study of gases at low concentrations like ethylene (Yahia et al., 2019). Microreactors have small volumes and precise controls that allow for optimal gas chromatography analysis. Compared to other analytical techniques such as fractional distillation and column chromatography, gas chromatography is generally carried out on a smaller scale, making it ideal for microreactors (Li & Lui, 2019). Pyrolysis has also been coupled with microreactor technology since as early as the 1960s for better analysis of thermal decomposition (Cox & Ellis, 1964). Noninvasive Raman spectroscopy can be performed in tandem with the microreactor, as the Raman spectrometer can directly analyze the small amounts of products that emerge from the microreactor (Mozharov, 2011).

1.2.2 Microreactor Application in Pharmaceuticals

An estimated 50% of current pharmaceutical reactions have the potential to benefit from implementation of microreactor technology (Roberge et al., 2005). Microreactors are especially useful for gas exchange reactions, gas/liquid, or liquid/liquid exchanges, which would be beneficial to the pharmaceutical industry. However, the lack of a solid interface is prohibitive to some processes. These types of reactors are particularly useful because of the high local heat density within microreactors, which can reduce reaction selectivity for specific products (Roberge

et al., 2005). Microreactors allow for safer handling of specific reactions because of the small volume of reactants used (Kockmann & Roberge, 2011). Since the pharmaceutical industry can be fast-moving, microreactors can be beneficial for competitive products that have a quick turnaround, which can reduce costs overall (Wong-Hawkes et al., 2007).

1.3 Green Chemistry

The concepts of Green Chemistry are becoming more prevalent in the chemical engineering industry, as companies and researchers look to minimize impact on the environment while improving process efficiency (Haswell & Watts, 2003). Green Chemistry is the idea that chemical processes should minimize negative damage on the environment. In 1998, Anastas and Warner wrote "Green Chemistry, Theory and Practice" which outlines 12 principles for Green Chemistry that could help the chemical industry become more environmentally conscious, sustainable, and safe. Microreactors alone can directly contribute towards the fulfillment of 6 of these goals: Atom Economy, Design for Energy Efficiency, Catalysis, Inherently Safer Chemistry for Accident Prevention, and Prevent Waste. The unique properties of microreactors lend themselves well to Green Chemistry.

Microreactors can offer higher yield of products, which is part of the Atom Economy principle, which states that processes should minimize wasted reactants when possible. The heat transfer rates of microreactors are generally better than standard reactor counterparts, which contributes to Design for Energy Efficiency. Wall-coating of tubular microreactors allows for the introduction of catalysts into processes, which follows the Catalysis principle. Microreactors have smaller volumes and are easily controlled, allowing for inherently safer chemistry for accident prevention. Waste can be prevented in microreactors through their overall better efficiency and yield.

1.4 Ammonia Decomposition Using Microreactors

Because microreactors offer a myriad of benefits for general reactions and because of the potential of hydrogen to be used as a replacement fuel, the goal of our project was to design and optimize a microreactor for ammonia decomposition. Ammonia decomposition can be carried out on a variety of catalysts, including Ru, Ir, Ni, Rh, Pt, Pd, Fe, Co, and a combination of other catalysts (Okura et al., 2016). Researchers have used catalytic microreactors, primarily microchannels, to examine the potential for hydrogen production. In our Major Qualifying Project, we developed a design for a microreactor through stainless steel tubing. This design was created through the development and characterization of a boehmite wall-coating with the intent to use incipient wetness impregnation to add Ni/Al2O3 catalyst to the coating. We simulated the heat transfer through our reactor design in order to determine the heat transfer properties through the system. At the end of this project, we wanted to develop a yield effective and cost effective microreactor that could be potentially scaled up for the local production of hydrogen.

Section 2: Technical Background and Literature Review

2.1 Properties of Microreactors

Microreactors are generally accepted to be channels or tubes made from glass, ceramics, steel, borosilicates, or other materials with diameters less than 1mm. Figure 1 shows a typical channel microreactor that can be used for a variety of purposes. There are hundreds of different large-scale reactors that have proven successful for many years, but microreactors have some advantages over traditional units.

Figure 1. A typical microchannel reactor that is etched into a stainless steel and glass apparatus (Amarequip, 2020).

Within these small reactors, chemical processes can occur rapidly because of fluid flow and heat and mass transfer. When looking at the fluid flow and mixing properties of the microreactor, it generally has the advantage over traditional reactors. Since microreactors have diameters less than a millimeter, the fluid flow generally is in the laminar region. Using the Reynolds number, most microreactors have a range of about 10-500, and anything under 2200 is considered to represent laminar flow. Since microreactors have a high surface area to volume ratio,

more thermal heat is able to diffuse out of the microreactor, making them ideal for exothermic reactions (Tanimu et al., 2017).

Microreactors have very short contact time with reactants, whereas many traditional reactors have several hours or days in contact with the reactants (Hessel, 2015). The types of reactions occurring in microreactors should be carefully considered, as some reaction chemistry will be more effective than others. A study by Lonza Company estimated that of 86 reactions, only 20% occurred rapidly enough for application in microreactors, but recent work shows that 80% of organic reactions can occur in a microreactor (Hessel, 2014).

2.2 Reactor Design

For heterogeneous gas-phase reactions, microstructured reactors can take the forms of plate or tubular reactors, with catalyst loading in the form of either packed bed or wall-coated. Microchannel plate reactors are usually metallic or ceramic plates with small parallel channels etched in (Ying et al., 2016). Packed bed microreactors are microchannels filled with solid catalyst; these are potentially superior to normal packed bed systems due to the high surface-to-volume ratio and therefore improved mass and heat transfer (Jensen, 2001). Wall-coated microreactors are able to lessen the effects of high pressure drops which typically occur in packed bed reactors (Kiwi-Minsker & Renken, 2005).

Stainless steel was chosen as the reactor substrate of interest over ceramics such as quartz because it has higher heat tolerance, mechanical strength, and thermal conductivity, along with relatively low cost (Novaković et al., 2008; Ying et al., 2016). One of the issues surrounding catalyst wall-coating stainless steel substrates is the difficulty in adhering the catalyst to the surface of the metal. Ceramic substrates are very porous, which allows for good adhesion of the catalyst; metals, however, tend to have smoother surfaces. To provide a rougher, more porous surface, the

metallic substrate usually needs to be pretreated and subsequently washcoated with a boehmite precursor sol gel (Laguna et al., 2016; Nijhuis et al., 2001). The boehmite precursor undergoes a phase transformation to γ-Al_2O_3 upon calcination, which provides a porous intermediate layer that allows for the catalyst slurry to bind better to the surface (Peela et al., 2009).

2.3 Wall-Coated Microreactors

Traditionally, packed bed reactors have been used for catalytic processes in which a reactant gas flows over solid catalyst pellets. Packed bed configurations tend to have heat transfer limitations, so the temperature of the reactor cannot be easily controlled. They also experience high pressure drops due to friction and poor geometry, especially if optimization of the catalyst particle sizes, reactor length, and ratio of reactor length to diameter does not occur (Ying et al., 2016). Further, mass transfer limitations manifest in packed bed reactors as channeling of the reactant in which the gas flows along the same path down the reactor, leaving some of the catalyst pellets unreacted (Bravo et al., 2004). These conditions may restrict the efficiency of the catalytic conversion process, prompting a need for a better reactor configuration.

2.4 Coating of Microreactors

2.4.1 Methods for Catalytic Wall-Coating of Microreactors

The first step in the coating process is pretreatment of the substrate. For metallic substrates, roughening the surface is necessary for improved catalyst adherence. The most commonly used methods are anodic oxidation, thermal oxidation, and chemical treatment. Anodic oxidation provides a direct current to an electrolytic substance in direct contact with an aluminum-containing metal to react and form a porous aluminum oxide layer. Thermal oxidation is a method that tends to be used on FeCrAl metals, which develops an aluminum oxide layer upon heating in air to

temperatures exceeding 800°C. Chemical treatment involves using dilute HCl, HNO_3, or a combination of both acids to clean and etch the metallic surface (Meille, 2006)

After the metal surface is treated, the catalyst support (boehmite precursor) is most commonly deposited as a suspension or sol on the surface via washcoating. The only notable differences when utilizing a sol gel over a suspension are the need for peptization of the sol precursor (boehmite, given the desired catalyst support is alumina) and the catalyst support is dissolved in a solvent prior to gelation (Meille, 2006; Nijhuis et al., 2001).

Catalysts can be coated on the surface in similar ways to those previously mentioned, with the added methods of electrophoretic deposition (EPD), electrochemical deposition, electroless plating, and impregnation. EPD involves applying a direct current to a colloidal suspension to favor migration of charged particles to another electrode. Electrochemical deposition is similar to EPD, but requires electrolysis of an ionic solution—usually a metal salt—to deposit a film on the surface of the substrate. Electroless plating also deposits a metal onto a substrate's surface, but uses a redox reaction instead of electrolysis. Impregnation deposits the catalyst by coating the substrate with a catalyst slurry which is subsequently calcined, leaving behind a thin catalyst layer (Meille, 2006).

2.4.2 Use of Boehmite for Wall Coating Applications

Boehmite is an aluminum oxyhydroxide, a crystalline mineral that is, in essence, a hydrated form of alumina, taking either the formula γ-AlOOH or $Al_2O_3 \cdot H_2O$ (Iijima et al., 2016). Figure 2 shows the networked boehmite as connected sheets.

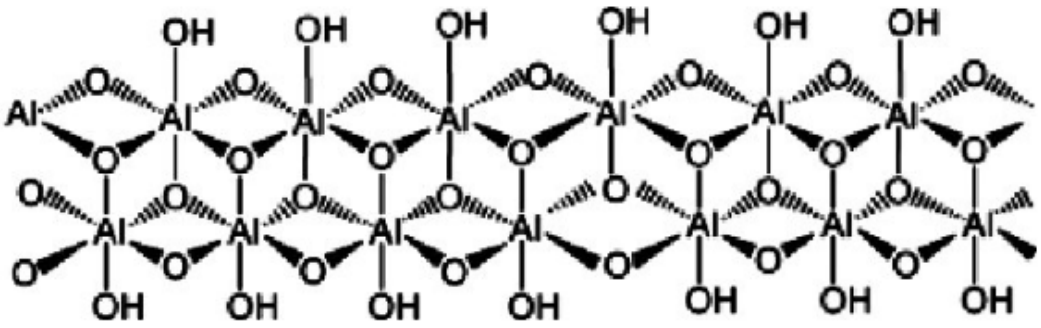

Figure 2. The boehmite structure as a connected network of sheets (Rajabi & Derakhshan, 2010).

At high temperatures, boehmite will dehydrate and convert first to γ-alumina and then to α-alumina, which is the most stable phase of alumina. The conversion to γ-alumina occurs at approximately 500℃ while achieving the α-alumina stable phase requires temperatures upward of 1000℃ (Lamouri et al., 2017). Figure 3 depicts the phase-change diagram of boehmite.

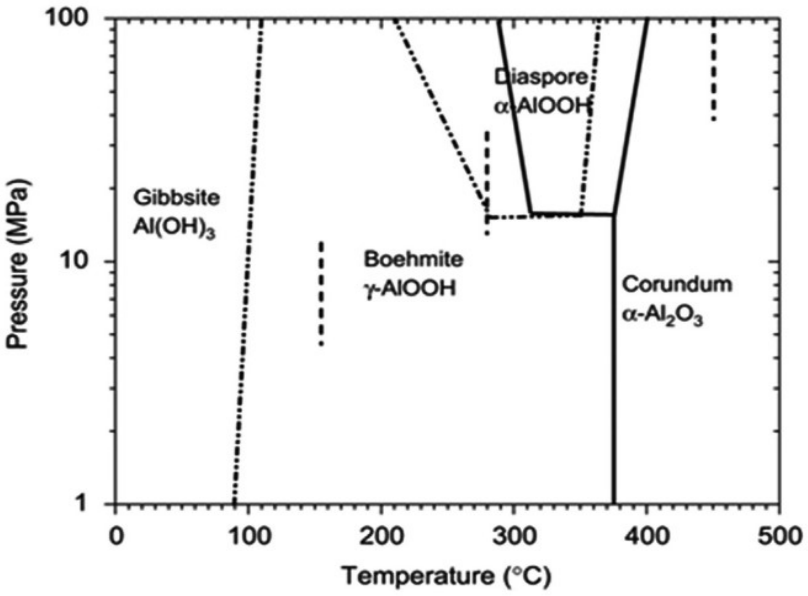

Figure 3. Phase diagram of boehmite and its transformations at various temperatures and pressures (Ghanizadeh et al., 2014).

The alumina formed from boehmite has a wide variety of uses and is incredibly versatile due to high strength, stability, and hardness at high temperatures (Panda et al., 2006). Boehmite itself is effectively used as a binder for the catalyst in the coating medium, as it transitions to alumina upon calcination of the coated surface. Boehmite increases the porosity of the coat, which improves the adhesion strength of the slurry to the surface, which in this case is stainless steel. Further, the addition of acid to a boehmite-water solution will increase viscosity which in turn increases the coating thickness on the surface (Bravo et al., 2004).

2.5 Catalysts for Ammonia Decomposition

There are various catalysts which may be used for ammonia decomposition, including iron, cobalt, nickel, copper, ruthenium, and iridium. Ruthenium and iridium tend to be the most active catalysts for the decomposition reaction, but are significantly more expensive than slightly less active alternatives like nickel. However, nickel has comparable hydrogen conversions to ruthenium and iridium so is therefore an attractive alternative (Boisen et al., 2005; Choudhary et al., 2001; Yin et al., 2004). Ultimately, the same catalysts that work best for ammonia synthesis are not always the best for ammonia decomposition

2.6 Reaction Kinetics for Ammonia Decomposition

In our research project, we use the reaction rate constant of ammonia decomposition to determine several dimensionless numbers to predict the flow and heat transfer regimes within our microreactor. The reaction kinetics and rate expressions for ammonia decomposition depend on a variety of factors. Unlike some other reactions, the rate expressions can change for ammonia decomposition based on the temperature of the reactor. A paper by Chellappa, Fischer, and Thomson states that a large number of ammonia decomposition reactions depend on the temperature of the reactor and the hydrogen partial pressures (2001). A summary of generally

accepted principles for hydrogen production from ammonia decomposition are summarized: at low temperature and hydrogen partial pressures, the decomposition reaction is zero order in terms of hydrogen, while decomposition reactions run at low temperatures and high hydrogen partial pressure will be a first order reaction with respect to ammonia (Chellappa et al., 2002). They further suggest that for high-concentration ammonia decomposition, the reaction should be run at temperatures greater than 500°C to minimize the effects of hydrogen inhibition that can occur at lower temperatures and pressures. A detailed explanation of the reaction rate constant used in our calculations can be found in the Results section of the paper.

2.6.1 Dimensionless Numbers in Microreactors

Because of their geometry, microreactors have unique flow and reaction properties. Within the microreactor, there are dimensionless numbers that can help predict flow regimes, mixing, and reaction kinetics. How these dimensionless numbers work together contribute to the unique properties of microreactors, such as desirable mixing, laminar flow, and having a kinetics-limited reaction rather than limited by heat transfer of the reactor. In this project, we specifically wanted to examine the relationship between the Biot Number and the Damkohler numbers, which can predict if the decomposition reaction within our microreactors would be kinetically limited or limited by the heat transfer of the reactor. In order to calculate the Biot and Damkohler numbers, additional dimensionless numbers are needed including the Reynolds number, Prandtl number, and Nusselt number.

2.6.2 Reynolds Number

The Reynolds number (Re) of a microreactor can predict the flow regime of a particular flow through pipes of various diameters. The dimensionless number is the ratio of the inertial forces to the viscous forces of the fluid, as seen in Equation 1.

$$Re = \frac{\rho u D}{\mu} \quad \text{Eq. 1}$$

The Reynolds number relies on the diameter of the tube, the dynamic viscosity of the fluid, the fluid speed, and the density of the fluid. When the resulting Reynolds number is larger, generally over 2,900, the fluid flow regime can be considered turbulent. If Re is less than 2,300, the flow is considered laminar, and Re between 2,300 and 2,900 are considered to be in a transitional regime. While the properties of the fluid vary between reactions and conditions, the diameter of the microchannel plays a large role in determining the flow regime (Chinnov et al., 2015).

2.6.3 Prandtl Number

The Prandtl number (Pr) is the ratio of the kinematic viscosity over the thermal diffusivity of the fluid, as shown in Equation 2.

$$Pr = \frac{u C_p}{k} \quad \text{Eq. 2}$$

Pr depends on the kinematic viscosity of the fluid, the specific heat capacity of the fluid, and the thermal conductivity of the fluid. The Prandtl number can be considered relatively constant for gases even at high temperatures, which makes it an ideal dimensionless number for the decomposition of ammonia through our microreactor design. The Prandtl number can be considered an intrinsic property of a fluid (Rapp, 2017). Like the Reynolds number, the Prandtl number can be used to determine other dimensionless numbers.

2.6.4 Nusselt Number

The Nusselt number (Nu) describes the relationship between the heat transfer of a fluid moving in a pipe to the solid pipe. It can also be described as the ratio of the convective heat transfer to the conductive heat transfer, as shown through Equation 3.

$$Nu = \frac{hD}{k} \quad \text{Eq 3.}$$

The Nusselt number can be calculated through the characteristic length of the system, D, in this case the thickness of the microreactor wall. It also depends on the heat transfer coefficient of the fluid and the thermal conductivity of the fluid. The Nusselt number can also be described through relationships between Re and Pr. Unlike Re and Pr, the equations used for the Nusselt number depend on geometry, flow regime, and heat transfer of the fluid. The main use of the Nusselt number in this study is to determine the heat transfer coefficient of the ammonia through our designed microreactor at specific operating conditions.

2.6.5 Biot Number

The Biot number (Bi) can be described as the ratio between the conductive and convective heat transfer of a system. A small Bi number indicates a thermal uniformity throughout the reactor. Equation 4 shows the equation used to calculate the Biot number

$$Bi = \frac{\tau_{conduction}}{\tau_{convection}} = \frac{h*L}{k} \qquad \text{Eq. 4}$$

Bi uses the thermal conductivity of the microreactor walls, the characteristic length L or the thickness of the reactor walls, and the heat transfer coefficient of the fluid as calculated by the Nu number. By calculating Re, Pr, and Nu, the heat transfer coefficient for the ammonia in the microreactor can be calculated.

2.6.6 Damkohler Numbers

The Damkohler number (Da) is the final dimensionless number used in this project to determine the relationship between kinetics and heat transfer within our designed microreactor. Da_I is the ratio of the reaction rate over the convective mass transport rate, while Da_{II} is the ratio of the reaction rate to the diffusive mass transfer rate. The expressions for both of the Damkohler numbers are shown in Equation 5 and 6:

$$Da_I = \frac{\tau_{reaction}}{\tau_{conduction}} = \frac{k}{\rho * C_p * L^2 * k_{reaction}} \quad \text{Eq. 5}$$

$$Da_{II} = \frac{\tau_{reaction}}{\tau_{convection}} = \frac{h}{\rho * C_p * L * k_{reaction}} \quad \text{Eq. 6}$$

The Damkohler number uses the reaction rate constant k, the thermal conductivity of the fluid, the density of the fluid, the specific heat of the fluid, and the characteristic thickness of the reactor tubing. Damkohler numbers less than 1 indicate that the microreactor is kinetically limited, while those larger than 1 indicate that the reaction is limited by heat transfer. The ratio of the Damkohler numbers becomes the Biot number, which makes these three dimensionless numbers useful in comparisons. The Damkohler numbers in conjunction with the Biot number can determine if our microreactor design can theoretically operate isothermally, as seen in Figure 4.

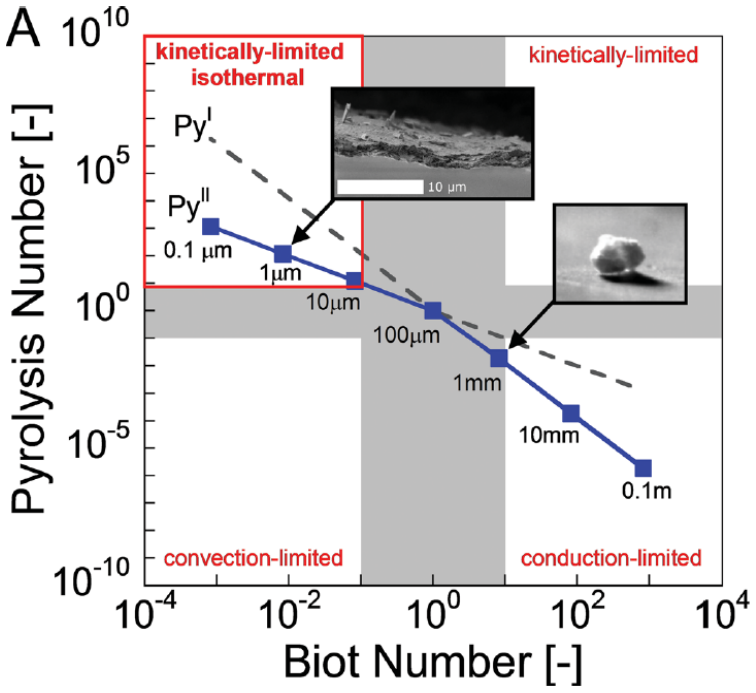

Figure 4. A graph showing the results of graphing the Pyrolysis numbers, which is the same as the Damkohler number in this case, against the Biot number for reactors of varying sizes (Mettler et al., 2012). Our target microreactor design would fall into the upper left section of the graph.

2.7 Heat Transfer Properties

Significant advantages of stainless steel microreactors with respect to heat transfer are the isothermal nature of them, along with their efficient heat transfer abilities (Bravo et al., 2004). Microreactors are also suitable for highly exothermic or endothermic reactions and allow for operation at more intense conditions (Kiwi-Minsker & Renken, 2005).

Section 3: Methodology

To prepare the best coating of boehmite into steel capillary microreactors, we ran several experiments. To achieve our goal of designing and optimizing a catalytic microreactor for the decomposition of ammonia, we developed 4 main steps for our methodology:

1. Thin Film Coating of Metal and Glass Slides
2. Characterization of Thin Film
3. Cylindrical Coating of Stainless Steel Microreactors
4. Mass and Heat Transport Modeling

Our first set of experiments tested boehmite gel coating on steel plates and wall-coating the inside of microreactors. We characterized the properties of the gel coating through X-ray diffraction and optical 3D profilometer. We simulated heat loss through a single and bundled capillary during ammonia decomposition using COMSOL modeling.

3.1 Section: Preparation and Characterization of Boehmite Gel

3.1.1 Initial Gel Preparation

Our control experiment polymerized boehmite without using a catalyst or any heating elements. Based on previous research and suggestions from researchers in the Teixeira laboratory, 0.5 grams of boehmite was added to a five-dram vial. 10 mL of deionized (DI) water was added to the boehmite, and the vial was capped and shaken until the boehmite was fully dissolved. Three three-dram vials were prepared using this method. With a disposable Pasteur pipette, ten drops, two drops, and no drops of concentrated 37% HCl were added to each dram, respectively. The contents of the dram vials were then mixed again for several minutes until gelation began to occur.

Observations were made immediately after polymerization and then again 24 hours later after the polymerization. We used paper pH strips to test the pH levels of the slurry after 24 hours.

3.1.2 Determining Acid Polymerization Threshold

To determine the amount of HCl needed to begin polymerization, we added increasing amounts of HCl to dram vials. Following the aforementioned procedure, we prepared nine three-dram vials with 0.5 grams boehmite and 10 mL of DI water. We then added increasing amounts of HCl to each dram, starting with three drops in dram 1, then four in dram 2, up to eleven drops in dram 9. Instead of a disposable glass Pasteur pipette, we used a bottle with a dropper cap to drop HCl into the boehmite solution. Appendix A shows the calculations for determining the amount of acid added per drop.

We mixed the contents in each vial for several minutes and recorded initial observations about viscosity. After 24 hours, we made more observations about the resulting polymerization viscosities and took pH readings using paper strips.

3.1.3 Pretreatment of Metal Substrates

Two different substrate geometries were utilized in this study:

(1) 0.03-inch-thick 304 stainless steel plates (McMaster-Carr) which were cut to approximate microscope slide dimensions of 1 inch by 3 inches.

(2) 304 stainless steel hypodermic tubes, 400um ID, 500um OD (Microgroup), approximately 2 inches in length

The steel substrates were pretreated to enhance the adhesion of the coating, as metals do not have prominent pores in which the boehmite gel can bond (Ma et al., 2019). Therefore, metals are not as common for use as microreactors, because adhesion of the boehmite after calcination—a ceramic, alumina—will not necessarily hold up.

The pretreatment was performed by placing the slides in a diluted HCl bath (~3%) for ten minutes at approximately 80 ± 10℃. DI water was used to wash off the HCl, and then the clean plates were placed in an acetone bath for thirty minutes. They were dried in an oven overnight at 120℃.

3.1.4 Coating Boehmite Gel on Metal Slides

Initially, 1 inch by 1 inch squares were sectioned off in each slide using autoclave tape available in the lab. We applied a thin coating of one of the slurry mixtures to the steel plates between the tape pieces and used a razor blade to level off the coating. This procedure was repeated with each of the slurry mixtures and at two tape thicknesses 0.147 mm and 0.254 mm (one and two pieces of autoclave tape). The metal plates were allowed to dry completely, and then the acid was removed from the slurry by running DI water over the dried mixture until the runoff water had a pH of 7. We then placed the metal slides into the oven overnight at 120℃.

3.2 Calcination and Characterization of Thin Films

3.2.1 Calcination of Boehmite on Metal Slides – XRD Confirmation

Improving on this previous method, plates were cut in half lengthwise to accommodate the tube furnace and coated in the same manner as outlined above. The plates were dried and loosely covered overnight at room temperature. Of the prepared slides, the slide that was treated with 9 drops of HCl and prepared with one layer of tape was calcined in flowing air at 500℃ for 3 hours with a ramp time of 45 minutes. Later, the adherence and consistency were tested.

3.2.2 Adherence and Consistency on Metal Slide – Optical Profilometry Confirmation

To test the properties of the slurry, we observed the overall adhesion to the plate. We initially weighed each slide before testing the adhesion properties, however, the mass measurements were not accurate enough to discern major differences. Adhesion was tested by

tapping the plates on the lab bench and observing the approximate amount of coating that fell off. Consistency of the coating was examined using the optical 3D profilometer in Washburn Shops.

3.3 Preparation of Stainless Steel Microreactors

3.3.1 Wall-Coating through Gas Displacement Method

The stainless steel tubes used in this experiment were purchased from Microgroup from Medway with a steel type of ##304H25XX. The tubes have an inner diameter of 400 micrometers and an outer diameter of 500 micrometers. The stainless steel tubes came in 1 ft lengths and were cut down using a handheld rotary tool to lengths of approximately 5.1 cm. These cut lengths of tubes were then subject to the same steel pretreatment method as outlined in section 3.1.3.

To coat the inside of the stainless steel tubes, a wall-coating method involving pressurized air. The general principle of this wall-coating technique is that pressurized air forces gel through the desired microreactor tube, which deposits a thin film of the gel along the interior of the tube. A schematic of the wall-coating apparatus can be seen in Figure 5 below.

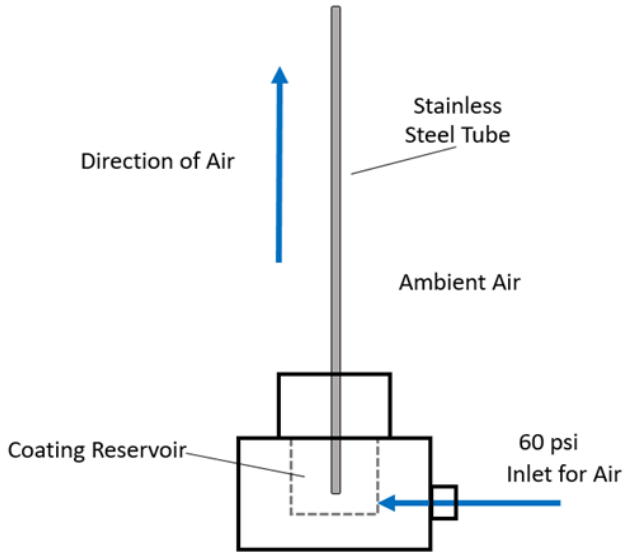

Figure 5. A schematic of the wall-coating apparatus used to add a thin coating of boehmite to the inside of the microreactors.

A small quantity of boehmite gel is loaded into a chamber with two openings. At the top opening, a prepared microtube is held in place so that its bottom portion is held within the gel reservoir while the top of the tube is open to the ambient air. The second opening feeds pressurized air at 60 psi into the side of the gel reservoir, which forces air through the gel and out through the tube. The air moves the gel along the inside of the tube, depositing a thin coating of the gel on the interior of the rube. This apparatus was constructed by Cameron Armstrong, a PhD candidate in Professor Teixeira's laboratory, for his own research.

3.3.2 Adding Rigidity to Microreactors for Analysis

To observe the thickness and adherence of the boehmite gel within the capillary tubes, we added rigidity to allow for a cross-sectional analysis. We melted paraffin wax around 70℃ and then added the coated capillaries to the wax for about 15 minutes to allow for the wax to be drawn inside. The tubes were then removed and cooled to room temperature.

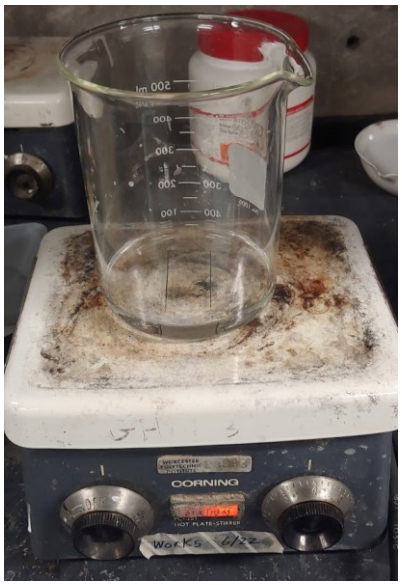

Figure 6. The coated capillaries were placed in melted paraffin wax to allow the wax to be drawn into the capillaries.

3.4 Decomposition of Ammonia in Microreactors

In the final stage of this project, we had intended to run ammonia decomposition reactions through the coated catalytic microreactors. Reactor conditions would have been varied to favor conversion to nitrogen and hydrogen gases, with a starting flow of 5 sccm at 500°C. The goal of this would have been to test 1) how effectively the catalyst was coated onto the inside of the reactor and 2) whether or not the chosen nickel-based catalyst could yield a reasonable conversion. Conversion would have been analyzed using a micro-gas chromatograph. Figure 7 below shows Armstrong's laboratory setup, which our reactor setup would follow.

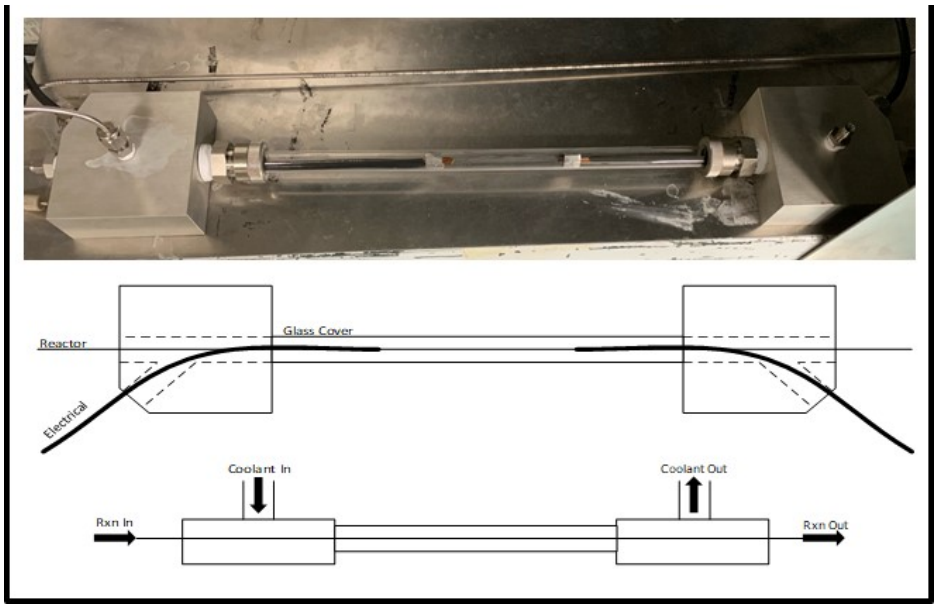

Figure 7. (Top) A photograph of a metal microreactor inside a quartz reacting aparatus. (Bottom) A schematic for the reactor design, showing the inlet and outlet for the coolant as well as the reaction flow direction. The reactor setup for a similar reactor. Ima

3.5 Modeling Heat Flux Through Microreactors

COMSOL Multiphysics was used to model the heat transfer through stainless steel microreactors in lieu of running ammonia decomposition reactions. A 1D axisymmetric model with heat transfer in solids was used. For simplicity, the alumina layer was considered negligible so the only solid was 304 stainless steel. The length of the reactor was assumed to be 1 meter, with an assumed velocity of 0.633 m/s (5 sccm). The heat transfer was specified as external forced convection at both points, with velocity inside the tube fixed and outside the tube variable; initial temperature and wall thickness were also variable in order to show how changing these parameters affects heat transfer. Initial temperature was assumed to be ambient (273.15 K) and pressure at 1 atm. Figure 8 below shows the 1D axisymmetric model, in which the wall thickness (left) is seen to be 50 nm and the right image shows the 2D cross-section of the tube. Parametric sweeps were run for initial temperature, external velocity, and wall thickness to show the heat transfer effects.

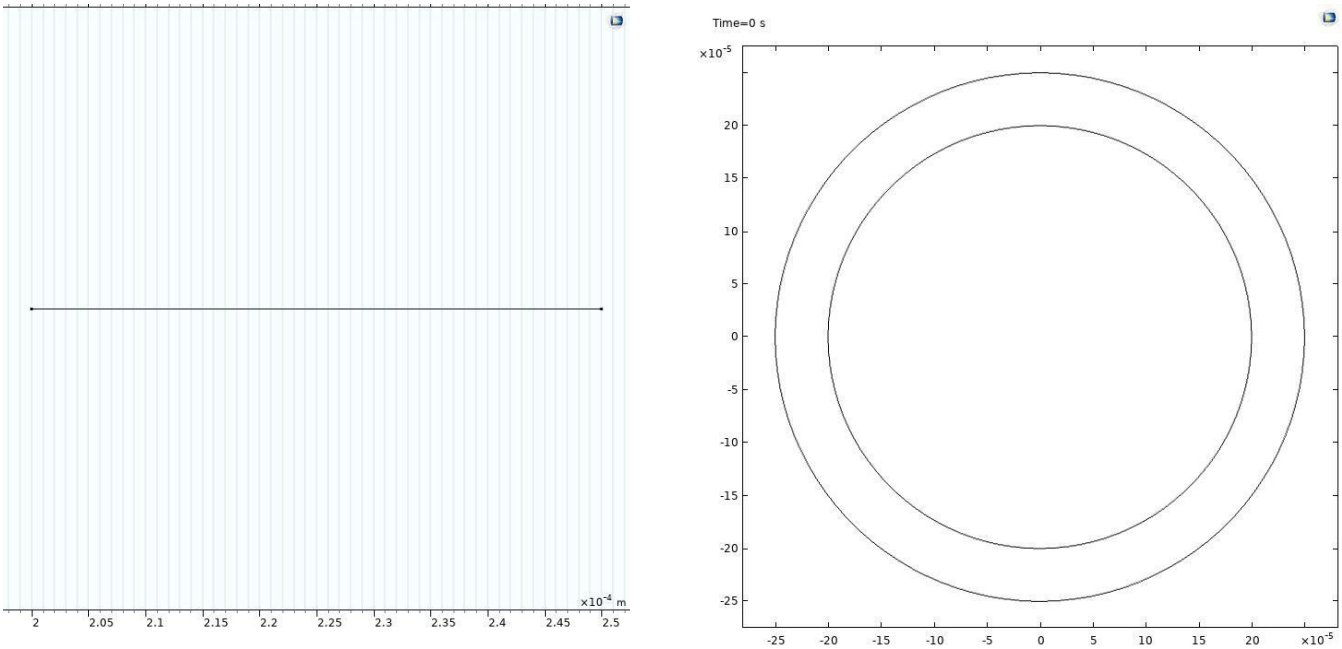

Figure 8. (Left) The wall thickness setup for the reactor system. (Right) The 2D cross section of the reactor tube.

Section 4: Results and Discussion

4.1 Development of Boehmite Thin Film Coatings

4.1.1 Gelation Point of Boehmite Coating

From our initial control trials, we determined that boehmite polymerization occurred with 10 drops of HCl. We determined the level of polymerization in this trial with observations about the viscosity of the resulting solution. The mixture that was just boehmite and DI water did not have any noticeable changes in viscosity. Since HCl was not present to initiate polymerization, we expected this result. In the original report detailing how to prepare and coat the tubes, Cameron Armstrong suggested using 2 or 3 drops of HCl to initiate polymerization. However, the boehmite required more HCl to initiate polymerization, as it came from an older stock. We confirmed these results in this initial control trial, as complete boehmite polymerization did not occur with only 3 drops of HCl. Figure 9 highlights the results of the polymerization without HCl.

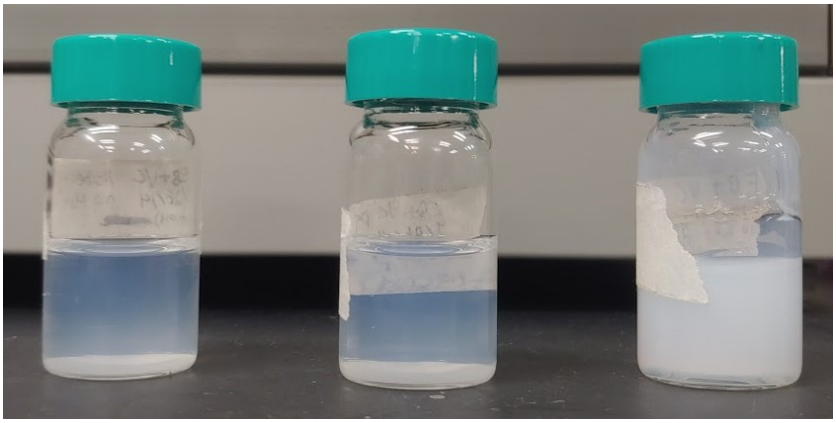

Figure 9. (Left to Right) Vials containing 0 drops, 3 drops, and 10 drops of concentrated HCl added to polymerize boehmite into a gel.

4.1.2 Determination of Acid Threshold for Gelation

After initial experimentation with boehmite gelation, we expected to find a specific amount of HCl needed to polymerize the boehmite. The boehmite gelled noticeably thicker at around the 6-7 drops of HCl range. In this experiment, we determined the amount of HCl needed for full polymerization of the boehmite. Immediately after the polymerization and 24 hours after polymerization, we observed the relative viscosities of each slurry (Figure 10). From our observations, the boehmite began polymerization after the addition of 7 drops of HCl, which corresponds to 315 µL added.

We noticed that the slurries appeared gel-like for the gels with drops 7-11 of HCl and could be inverted with little running. However, when the vials were agitated, the slurry would turn back into liquid. We suspect the boehmite gels exhibit shear thinning properties, as they became more viscous while under application of force, and then would reform into the original viscous gels after the force was removed and time had passed.

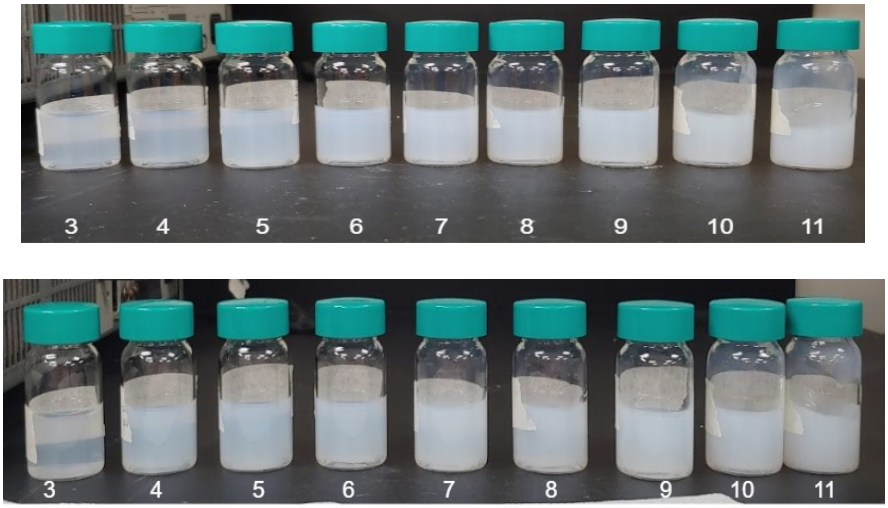

Figure 10. (Top) Boehmite immediately after polymerization with concentrated HCl. (Bottom) Boehmite 24 hours after polymerization with HCl. Numbers at bottom of image indicate number of drops of HCl added.

4.1.3 Determination of pH of Boehmite Gel

Since there was a noticeable difference between the viscosities of the gels depending on the amount of HCl added, we wanted to determine if there was a pH threshold that gelation occurred. We also determined the pH of each slurry using paper pH strips. However, all of the gels tested as the lowest pH possible on the scale, so we were not able to determine a threshold pH for gelation. A more precise pH digital reader may provide more insight about the pH variation between the gels.

4.2 Thin Film Coating of Steel Plates

4.2.1 Subsection: Initial Coating

After finding a range of viscous boehmite gels, we began refining our coating process on 2D plates. We ran initial coating trials with the gel from the 7-11 drops of HCl at 0.147mm and 0.254 mm thickness. After drying in the oven, we observed the coatings on all of the plates appeared clear and uniformly distributed across the plate (Figure 11)

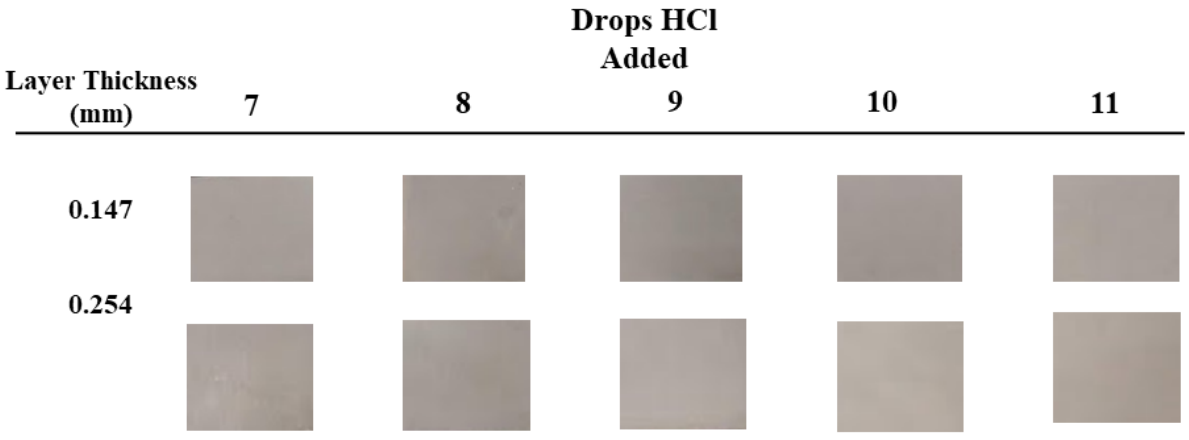

Figure 11. The initial trial of coating the plates with boehmite gels showed uniform coatings and colors, independent of the amount of HCl added to each gel.

4.2.2 Replicating Coating of Thin Film Plates

After our initial observations coating the plates, we replicated our experiment after creating a fresh batch of boehmite gels following the same procedure as before. The plates were dried and placed into an oven overnight. After the plates were removed from the oven, they sat loosely covered for several days. At the end of several days, the coatings on the plates turned orange and began flaking off of the slides (Figure 12). The flakiness increased in the gels that were prepared with higher amounts of HCl and were made at 0.254 mm thickness. Some of the flakes washed off of the plates using DI, but the flakes remained in the water.

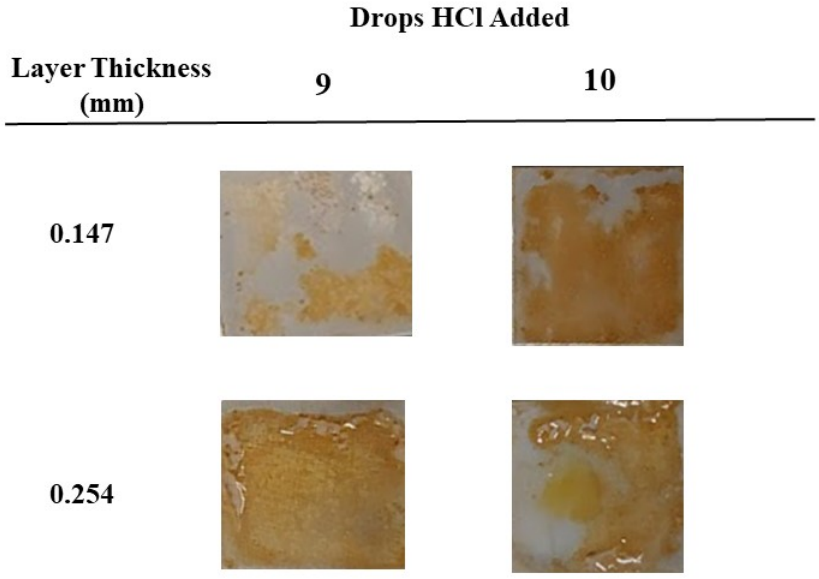

Figure 12. These are the slides coated with freshly prepared boehmite gel as outlined in the procedure. The plates show significant flaking after being left covered for several nights.

4.2 Thin Film Coating on Glass Slides

To determine the cause for the yellowing of the boehmite gel, we also deposited a thin film using the same thin film procedure for the steel plates. The resulting coatings were comparable for the same amount of HCl added and thickness of coating. Flaking was more common in the thicker layers of boehmite, the same as the steel coated plates (Figure 13).

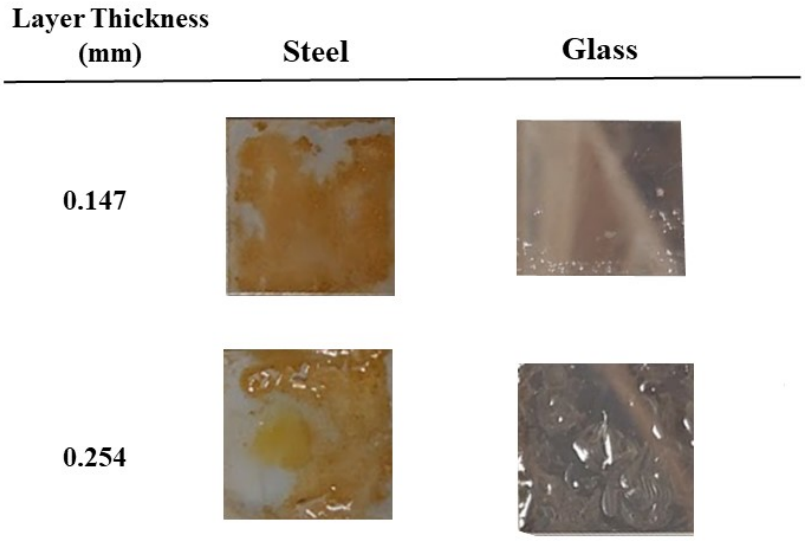

Figure 13. The slides prepared with 10 drops of HCl boehmite gel. Both sets of slides were dried overnight in the oven, and both slides show similar flaking. There was no color present in the boehmite coating on the glass slides, while the coating turned orange for the steel slides.

We suspect the boehmite coating became flaky partially because of buckling from the furnace. Because the flakiness occurred most with the thicker layers of boehmite, it is possible that excess boehmite that does not adhere to the plate will flake when water evaporates out.

There was no observable yellowing of the boehmite gels on the glass slides. This leads us to believe that the iron ions from the steel slides leeched into the boehmite gel which caused oxidation. This occurred in the slides that were left overnight in an air-circulating oven. To combat

the oxidation, we suggest placing coated slides into a furnace immediately after preparation. We suspect that if the furnace runs nitrogen over the samples, rather than oxygen-containing air, the boehmite coating may not oxidize.

We also noted that the slides seemed to oxidize faster and to a greater extent when prepared with boehmite gels that were fresh. When we coated the slides with gel that had aged more than a week, there seemed to be less oxidation.

4.3 Calcination and Characterization of Coated Slides

4.3.1 Preparation of Slides to be Calcined

To calcine our slides in the tube furnace, we repeated our process of coating slides with freshly prepared boehmite gels onto steel plates of 0.5 in width. Our initial slides immediately after preparation showed uniform color and coating, but after drying overnight, the slides showed some faint yellowing and flaking. As we determined from the glass slides, the yellowing is due to oxidation. Once the slides were placed into the furnace overnight, the 10 drops of HCl slides showed significant yellowing compared to the gel made with 9 drops of HCl. Figure 14 shows the progression of the slides from freshly prepared, dried overnight, and then after drying in the oven.

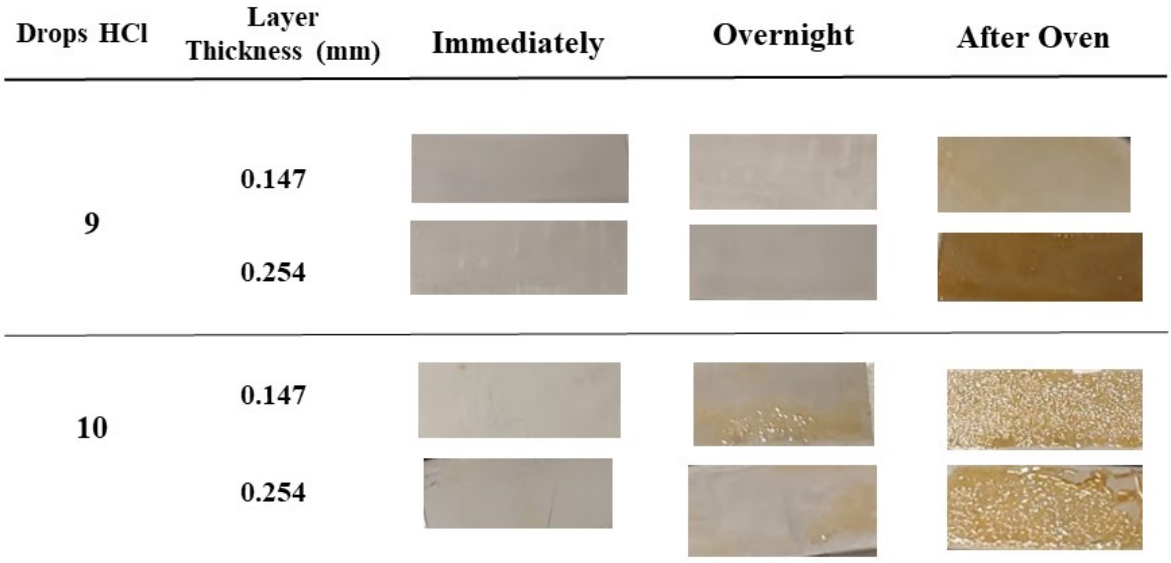

Figure 14. This image shows the progression of the flaking and color of the thin films prepared with 9 and 10 drops of HCl. The first column shows the slide coatings immediately after preparation. The middle column shows the films after sitting loosely covered overnight. The right column shows the films after left drying in the oven for 24 hours.

4.3.2 Calcination of Thin Film Coated Slides

We calcined the slide that was treated with 9 drop HCl applied at 0.147 mm thickness. This coated slide showed the least flaking and yellowing of the slides we prepared. After calcination, the slide showed discoloration throughout, and the coating became a darker orange color. Figure 15 highlights the differences between the slide after calcination.

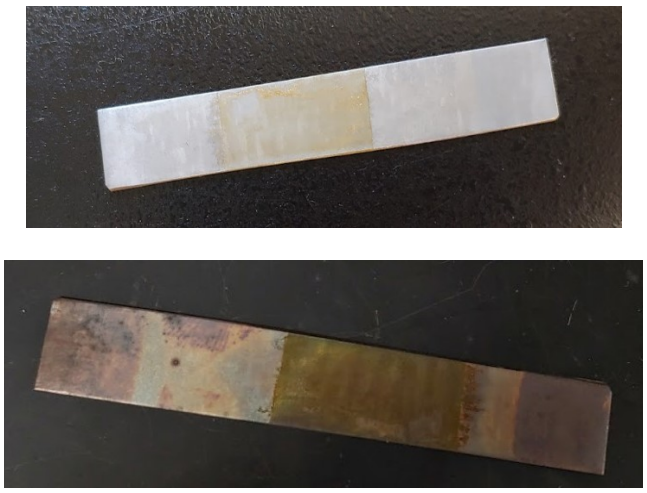

Figure 15. (Top) The coated slide that was treated with 9 drop HCl boehmite gel before calcination. (Bottom) The same slide after calcination at 550 C. The entire slide discolored, and the coated section darkened to a stronger orange color.

The thin film coating on the calcined slide darkened slightly, but otherwise remained visually the same as before calcination. Because the steel plates were pretreated to allow for better adhesion of the metal, the slides are easily oxidized at higher temperatures and discolor more readily. On different slides, we observed fingerprints were etched into the slide after going through the steel treatment process.

4.3.4 XRD Data of Calcined Boehmite

X-ray powder diffraction was utilized to validate the calcination methodology, ensuring that on heating to 500℃ for about four hours the boehmite would change phases to (gamma) alumina, Al_2O_3. Figure 16 shows the boehmite in the crucible before and after calcination.

Figure 16. (Top) The fresh boehmite powder before calcination treatment at 550 C. (Bottom) The calcined boehmite powder, while it seems more yellow in the photo, is due to ambient light.

To analyze the phase changes, the data points from the XRD readings were run through Jade software. The Jade software was able to identify the characteristic peaks of fresh boehmite that typically occur around 10, 20, 35, and 45, as shown in Figure 17.

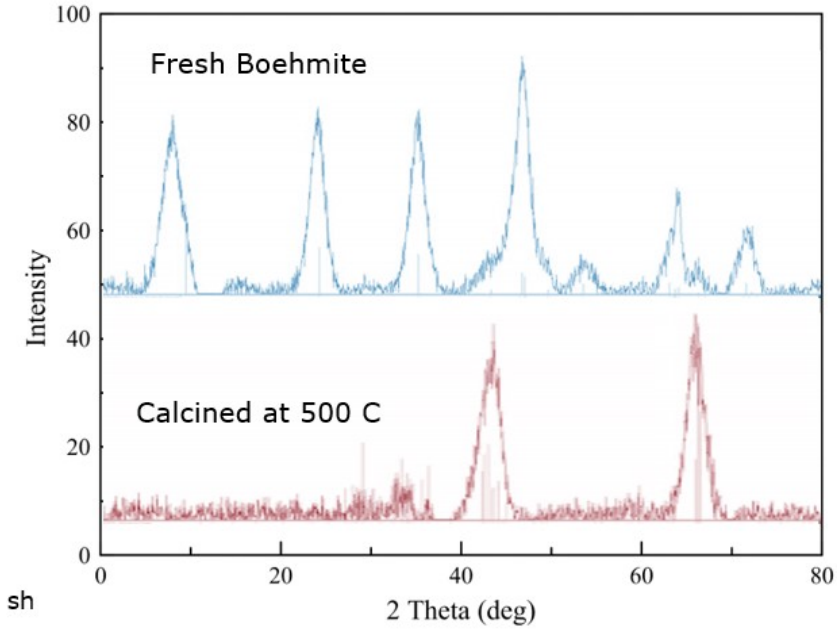

Figure 17. The XRD patterns for fresh and calcined boehmite powder. The faint vertical lines on each curve are the expected peak locations from Jade software.

The calcined powder subsequently shows two strong characteristic peaks around 40 and 65 with more noise than seen in the fresh boehmite powder. Within Figure 17, the faint vertical lines within each peak show where the Jade software would expect the peaks to appear. When compared to the predicted peaks from Jade, the fresh boehmite peaks matched the expected values better. The calcined boehmite has more noise in the XRD, and there are a few places the Jade software predicted a higher, more defined peak, like at 50 theta. The difference in predicted peaks and the actual peaks could be that the gamma translation did not fully occur. The boehmite powder was placed into a ceramic crucible at a depth of 1 cm, so the developed calcination treatment for the thin film on steel may not be as effective for the powder in the crucible. XRD confirming the phase change of the boehmite on the steel plate was planned, but was unable to occur due to campus closing.

4.3.5 Optical 3D Profilometry of Calcined Slide

We examined the consistency and thickness of the calcined slide coating using optical profilometry. Figure 18 below shows the profilometry image of the calcined slide. The darker left side of the image shows the steel plate. The darker line shows the split between where the coat was placed and the clean metal. The thin film is not entirely uniform, as shown by the small dark spots on the right side of the image. This was expected as the excess gel was scraped off with a razor, and the slide may have experienced some mild abrasion, which can explain the inconsistencies the coating.

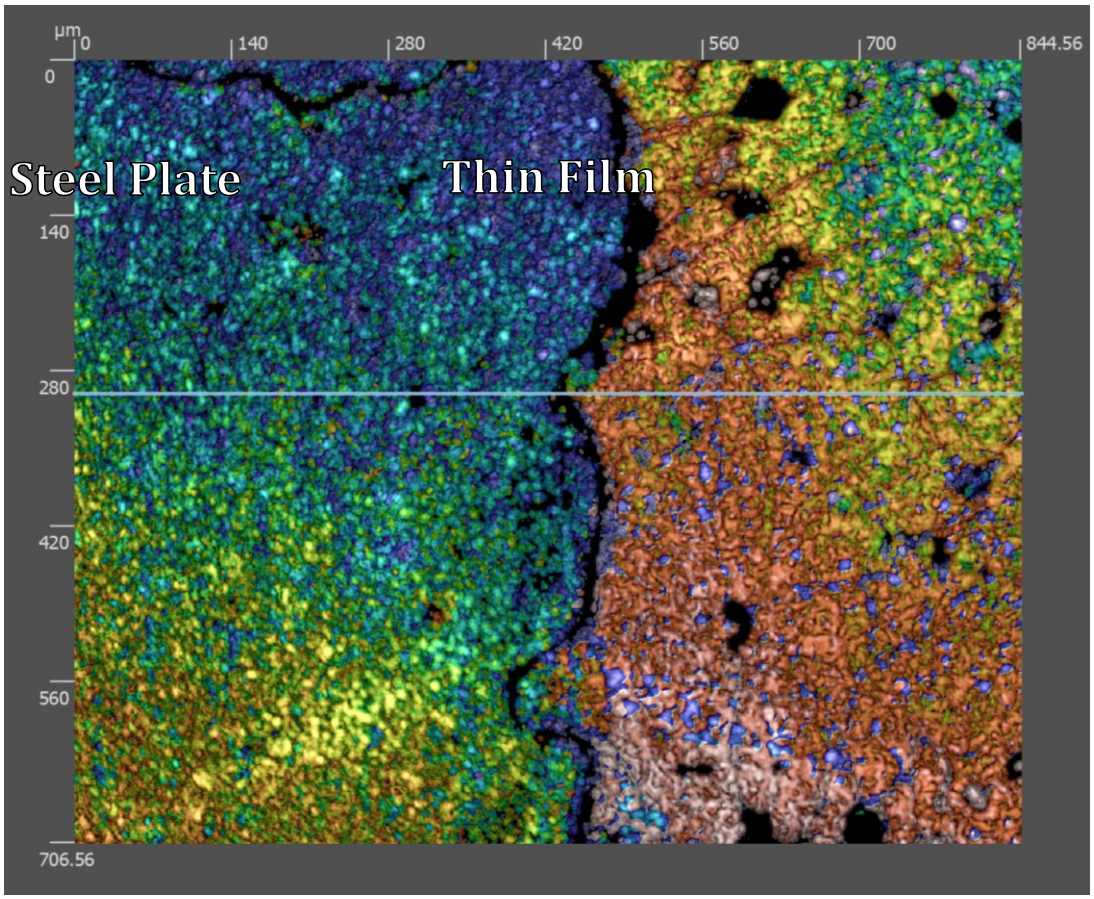

Figure 18. This colorized optical profile shows the lowest points in dark blue/indigo and the highest points in red. The light blue line at 280 µm shows where the depth readings were taken.

Figure 18 is the accompanying depth reading of the slide, which was taken at the thin blue reading line at around 280 µm in Figure 19. The graph shows the depth along the blue line. Once the profilometry reading reaches the thin coating, a sudden spike is seen on the graph at about 420 microns on the x axis reading. From the average readings, the graph shows the thin coating is approximately 1-2um thick, which was our target thickness. Although the coating started out at as 0.147 mm, the calcination burned off excess boehmite gel to leave behind the finished coating. The viscosity of the gel at 9 drops HCl shows to produce an ideal thickness, as it gives enough space within our tubular microreactors to add catalyst in a later step.

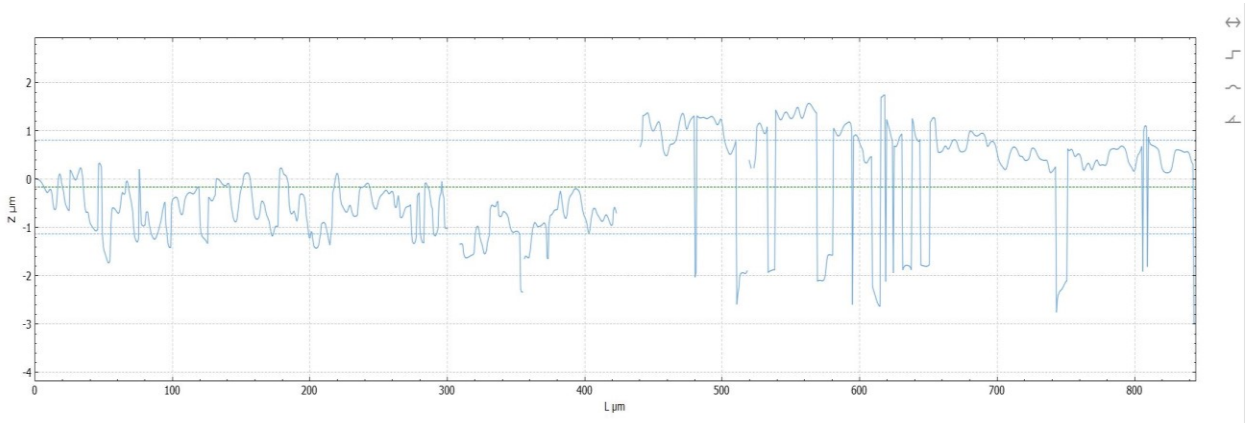

Figure 19. The chart shows the depth reading of the calcined slide along the blue line in Figure 19. The readings demonstrate an average coating thickness of about 1-2 micrometers.

4.4 Decomposition of Ammonia in Microreactors

Due to the ongoing worldwide COVID-19 pandemic, we were unable to actually run reactions in the lab. As an alternative, we modeled the mass and heat transfer of the system.

4.5 Biot and Damkohler Flow Regimes

The Biot number and the Damkohler numbers were used to predict the flow and heat transfer regimes through our designed microreactors. For our calculations, we made several assumptions based on our original operating conditions and advice from Cameron Armstrong. Our first assumption was that this reaction would take place at about 450°C. This operating temperature is slightly below our intended operating conditions but ran calculations at this temperature because of available values in literature. This section highlights important key assumptions made to produce the Biot and Damkohler plots, but Appendix B contains detailed sample calculations for the Prandtl Number, Nusselt Number, Biot Number, and Damkohler numbers.

4.5.1 Nusselt Number Relationship Determination

We selected a Nusselt number relationship between Pr and Re based on the resulting values and the geometry of fluid through a cylindrical tube. We selected Equation 7 shown below for the relationship

$$Nu = c * Re^{m} * Pr^{1/3} \quad \text{Eq. 7}$$

Equation constants c and m were determined based on the values of Re and Pr; because Re was less than 4 and Pr was greater than 0.7 for each thickness, c constant was 0.989 and m constant was 0.333. These values calculated the Nu number, which in turn helped determine the heat transfer coefficient of ammonia gas as 275.3 W/m^2*K. This calculated value is similar to heat transfer coefficients of gases housed inside of tubes, which was confirmation that our initial assumptions were correct.

4.5.2 Determining Reaction Constant of Ammonia Decomposition

We assumed a conversion rate of about 50% ammonia based on our temperature and similar experimental results of catalytic ammonia decomposition (Wang et al., 1999). From that conversion rate, we were able to use Arrhenius equation assumptions for ammonia decomposition to find the reaction constant needed for the Damkohler numbers.

4.5.3 Analysis of Biot Number and Damkohler Numbers Plot

To create our plot, we varied the thickness of our microreactor walls from 5 μm to 0.5 meters. Heat released during the exothermic ammonia decomposition reaction, so this plot could determine if kinetics or heat transfer properties limited our reactor wall thickness. Using the dimensionless numbers outlined in our methodology, we plotted the Damkohler numbers against the corresponding Biot numbers on a logarithmic scale, as shown in Figure 20.

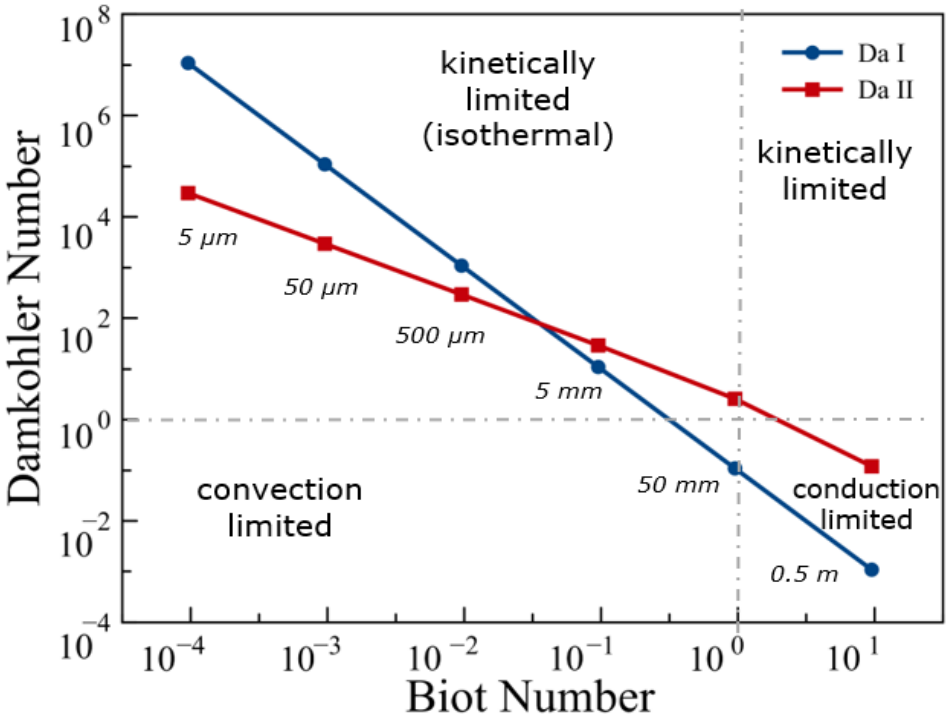

Figure 20. By varying the thickness of reactor walls, a plot of the Biot number vs the Damkohler numbers was created to determine the dominating kinetics/heat transfer for wall thicknesses.

When the Damkohler numbers are less than 1, it indicates that the wall thickness limits the conversion of ammonia in the reactor. When the wall becomes relatively thick compared to the operating space within the reactor, the heat generated from the ammonia decomposition takes longer to be removed, thus limiting the production of hydrogen. When the Damkohler number is larger than 1, the conversion of ammonia into hydrogen is limited by the kinetics of the reaction, rather than the heat transfer of the system. A Biot number larger than 1 indicates that the reactor system is limited by the rate at which heat can pass through the reactor walls. The reactors with wall thicknesses greater than 50 mm will be limited by the amount of heat that can pass through the walls of the system, which means it is conduction limited. However, a Biot number less than 1 shows that the heat removal from the system is limited by the convection of the ammonia within the reactor.

For our reactor design of wall thickness of 50 μm, we determined that it would be kinetically limited and isothermal. This is what we expected based on our research, as our reactor walls are thin enough to be limited by reaction kinetics rather than heat transfer. Additionally, since the Biot number is less than one for our 50 μm walled reactor, we can assume that the reactor will be isothermal. A small Biot number indicates less variation of temperature within the reactor, which confirms our goal of designing a reactor that is thermally effective.

4.6 Modeling Heat Flux Through Microreactors

Parametric sweeps were run to show how the variation of initial temperature, external fluid velocity, and wall thickness may affect how quickly the microreactor is able to cool down from a given temperature. The temperature sweep was run from 273.15 K to 800 K at an interval of 10 K. The velocity sweep was run from 0 to 10 m/s at an interval of 1 m/s. The wall thickness sweep was run at an exponential interval and plotted on a $\log_{10}$ scale: 5 μm, 7 μm, 9 μm, 50 μm, 70 μm,

90 µm, 500 µm, 700 µm, 0.5 cm, 5 cm. Each parametric sweep was run at a time step of 5 seconds from 0 to 100 seconds. From Figure 21 below, as the initial temperature of the system increases, the time it takes to cool to ambient temperature also increases as there is a larger temperature differential. In Figure 22, as velocity increases from 0 to 10 m/s, the time it takes to cool to ambient decreases as there is an increase in convective flow. In Figure 23, as wall thickness increases, the time to cool to ambient increases

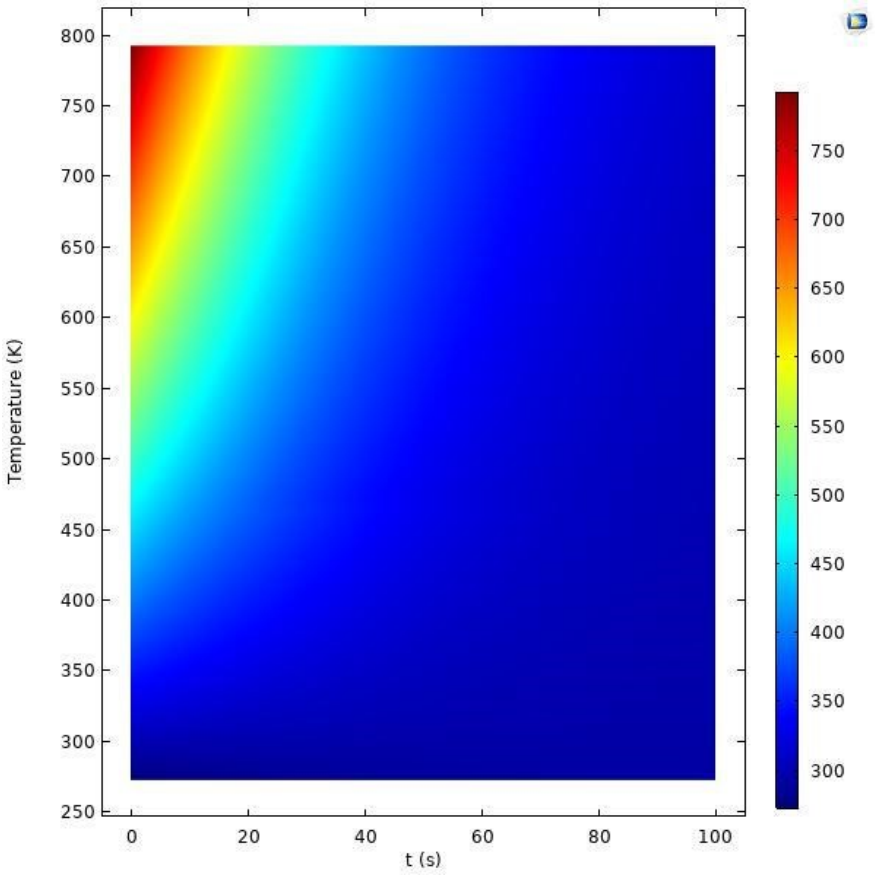

Figure 21. COMSOL plot of varying initial temperature with time as the average temperature of the reactor decreases.

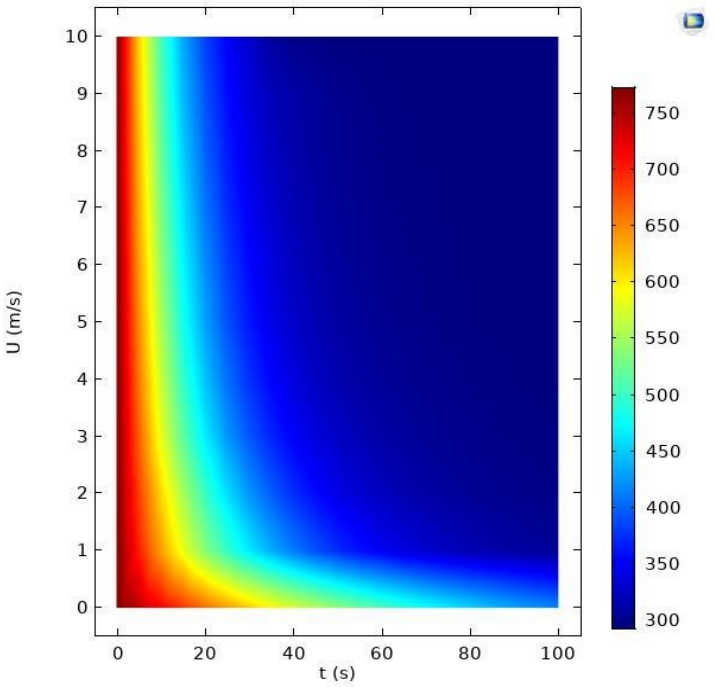

Figure 22. COMSOL plot of varying velocity with time as the average temperature of the reactor decreases.

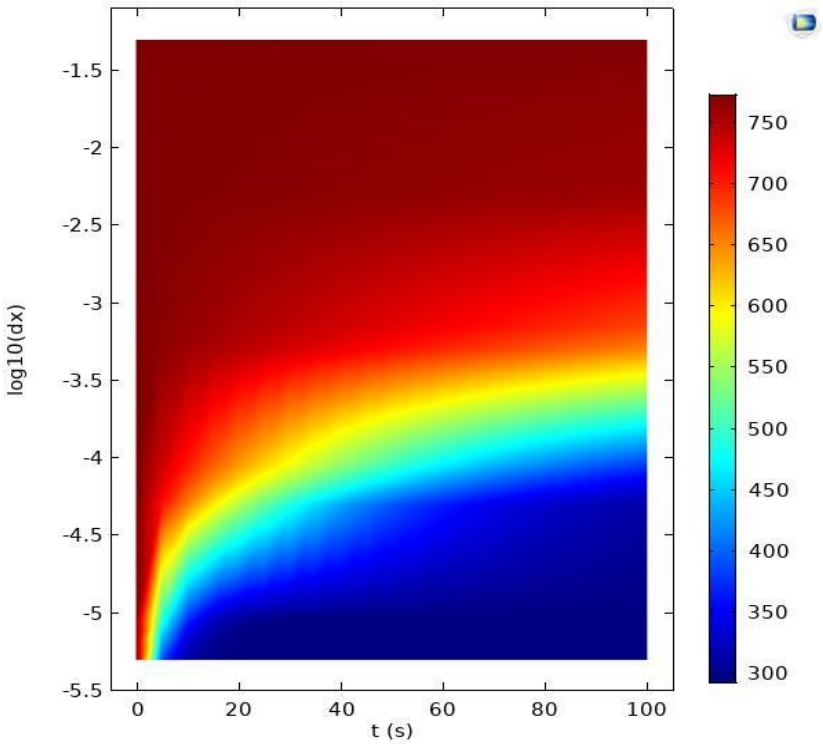

Figure 23. COMSOL plot of varying the log base-10 of thickness with time as the average temperature of the reactor decreases.

Section 5: Conclusions and Suggestions for Future Work

Ultimately, thin films can be successfully coated on 304 stainless steel plates and microreactors using the aforementioned methodology. Characterization of the thin films confirmed the desired phase change of boehmite into alumina. The desired thin film coating of 1 micrometer was achieved on the steel plates, as revealed by optical profilometry. The thin film coating method can be improved in the future potentially by coating the reactors in an inert atmosphere to prevent the yellowing of the steel. Further, we have shown that stainless steel microreactors have superior thermal properties over ceramic substrates, along with improved heat and mass transfer. Lastly, we have applied reaction engineering and dimensionless analysis to identify the isothermal and kinetic operating regime in order to demonstrate the most effective operating conditions for a tubular microreactor. From the COMSOL modeling, we suggest operating conditions of greater than 500 oC, which would provide a higher conversion rate of ammonia, while also allowing for less temperature variation within the reactor. To achieve a isothermal, kinetically limited reactor system with a nickel catalyst, the walls of the reactor should be no thicker than 500 μm, based on dimensionless parameters and confirmed with COMSOL modeling. While the velocity of the ammonia gas through the system can vary, a lower velocity of gas will cause a longer cool down time for the reactor system.

Because the final stages of testing the microreactors for ammonia decomposition did not occur due to campus closure, we suggest future research obtain proof of concept for the microreactor design. Without the campus closure, we planned to test the microreactors to obtain experimental yields for hydrogen. From those results, operating conditions could be suggested for the microreactor. In subsequent research studies, reactor design scale-up should be considered; the catalytic conversion of the reactant, i.e. ammonia to hydrogen and nitrogen gas, may be

significantly enhanced as opposed to traditional packed bed reactors for industrial purposes. Finally, this project assumed nontransient and isothermal conditions for the ammonia decomposition reaction. Studying more transient and nonisothermal reactor operations would provide a fuller picture of the feasibility of decomposition ammonia using catalytic microreactors as an alternative source for hydrogen.

References

What Is Green Chemistry? (n.d.). https://www.acs.org/content/acs/en/greenchemistry/what-is-green-chemistry.html

Abashar, M. E. E. (2018). Ultra-clean hydrogen production by ammonia decomposition. Journal of King Saud University - Engineering Sciences, 30(1), 2–11. https://doi.org/10.1016/j.jksues.2016.01.002

Adiya, Z. I. S. G., Dupont, V., & Mahmud, T. (2017). Effect of hydrocarbon fractions, N2 and CO2 in feed gas on hydrogen production using sorption enhanced steam reforming: Thermodynamic analysis. *International Journal of Hydrogen Energy*, *42*(34), 21704–21718. https://doi.org/10.1016/j.ijhydene.2017.06.169

Anastas, P., & Warner, J. (n.d.). 12 Principles of Green Chemistry. https://www.acs.org/content/acs/en/greenchemistry/principles/12-principles-of-green-chemistry.html

Boisen, A., Dahl, S., Nørskov, J. K., & Christensen, C. H. (2005). Why the optimal ammonia synthesis catalyst is not the optimal ammonia decomposition catalyst. *Journal of Catalysis*, *230*(2), 309–312. https://doi.org/10.1016/j.jcat.2004.12.013

Bravo, J., Karim, A., Conant, T., Lopez, G. P., & Datye, A. (2004). Wall coating of a CuO/ZnO/Al2O3 methanol steam reforming catalyst for micro-channel reformers. *Chemical Engineering Journal*, *101*(1–3), 113–121. https://doi.org/10.1016/j.cej.2004.01.011

Chellappa, A. S., Fischer, C. M., & Thomson, W. J. (2002). Ammonia decomposition kinetics over Ni-Pt/Al2O3 for PEM fuel cell applications. *Applied Catalysis A: General*, *227*(1–2), 231–240. https://doi.org/10.1016/S0926-860X(01)00941-3

Chinnov, E. A., Ron'shin, F. V., & Kabov, O. A. (2015). Regimes of two-phase flow in micro- and minichannels (review). *Thermophysics and Aeromechanics*, *22*(3), 265–284. https://doi.org/10.1134/S0869864315030014

Choudhary, T. V., Sivadinarayana, C., & Goodman, D. W. (2001). Catalytic ammonia decomposition: COx-free hydrogen production for fuel cell applications. *Catalysis Letters*, *72*(3–4), 197–201. https://doi.org/10.1023/A:1009023825549

Cox, B. C., & Ellis, B. (1964). A Microreactor-Gas Chromatographic Method for the Identification of Polymeric Materials. *Analytical Chemistry*, *36*(1), 90–96. https://doi.org/10.1021/ac60207a028

Dincer, I., & Acar, C. (2014). Review and evaluation of hydrogen production methods for better sustainability. *International Journal of Hydrogen Energy*, *40*(34), 11094–11111. https://doi.org/10.1016/j.ijhydene.2014.12.035

Dubey, S. P., Dwivedi, A. D., Sillanpää, M., Lee, H., Kwon, Y. N., & Lee, C. (2017). Adsorption of As(V) by boehmite and alumina of different morphologies prepared under hydrothermal conditions. Chemosphere, 169(February), 99–106. https://doi.org/10.1016/j.chemosphere.2016.11.052

Emmett, P. H., & Kummer, J. T. (1943). Kinetics of Ammonia Synthesis. Industrial & Engineering Chemistry, 35(6), 677–683. https://doi.org/10.1021/ie50402a012

Ghanizadeh, S., Bao, X., Vaidhyanathan, B., & Binner, J. (2014). Synthesis of nano α-alumina powders using hydrothermal and precipitation routes: A comparative study. *Ceramics International*, *40*(1 PART B), 1311–1319. https://doi.org/10.1016/j.ceramint.2013.07.011

Haswell, S. J., & Watts, P. (2003). Green chemistry: Synthesis in micro reactors. *Green Chemistry*, *5*(2), 240–249. https://doi.org/10.1039/b210539j

Hessel, V. (2015). Special issue: Design and Engineering of microreactor and Smart-Scaled Flow Processes. *Processes*, *3*(1), 19–22. https://doi.org/10.3390/pr3010019

Iijima, S., Yumura, T., & Liu, Z. (2016). One-dimensional nanowires of pseudoboehmite (aluminum oxyhydroxide γ-AlOOH). *Proceedings of the National Academy of Sciences*, *113*(42), 11759–11764. https://doi.org/10.1073/PNAS.1614059113

Jensen, K. F. (2001). Microreaction engineering - is small better? *Chemical Engineering Science*, *56*, 293–303.

Kiwi-Minsker, L., & Renken, A. (2005). Microstructured reactors for catalytic reactions. *Catalysis Today*, *110*(1–2), 2–14. https://doi.org/10.1016/j.cattod.2005.09.011

Kockmann, N., & Roberge, D. M. (2011). Scale-up concept for modular microstructured reactors based on mixing, heat transfer, and reactor safety. *Chemical Engineering and Processing: Process Intensification*, *50*(10), 1017–1026. https://doi.org/10.1016/j.cep.2011.05.021

Krietsch Boerner, L. (2019). Industrial ammonia production emits more CO2 than any other chemical-making reaction. Chemists want to change that. Chemical & Engineering News, 97(24).

Kuo, C. H., Yuan, F., & Hill, D. O. (1997). Kinetics of Oxidation of Ammonia in Solutions Containing Ozone with or without Hydrogen Peroxide. Industrial and Engineering Chemistry Research, 36(10), 4108–4113. https://doi.org/10.1021/ie9702082

Laguna, O. H., Domínguez, M. I., Centeno, M. A., & Odriozola, J. A. (2016). Catalysts on Metallic Surfaces: Monoliths and Microreactors. In *New materials for catalytic applications* (Issue December). Elsevier B.V. https://doi.org/10.1016/B978-0-444-63587-7/00004-4

Lamouri, S., Hamidouche, M., Bouaouadja, N., Belhouchet, H., Garnier, V., Fantozzi, G., & Trelkat, J. F. (2017). Control of the γ-alumina to α-alumina phase transformation for an

optimized alumina densification. *Boletin de La Sociedad Espanola de Ceramica y Vidrio*, *56*(2), 47–54. https://doi.org/10.1016/j.bsecv.2016.10.001

Li, D., & Liu, S. (2019). Drinking Water Detection. *Water Quality Monitoring and Management*, 251–267. https://doi.org/10.1016/b978-0-12-811330-1.00010-7

Ma, C., Luo, Y., Sun, B., Su, M., & Chu, G. (2019). Efficient Coating Method via Matching Rough Surface of Stainless Steel with Al2O3 Particles [Research-article]. *Industrial & Engineering Chemistry Research*, *58*, 1848–1856. https://doi.org/10.1021/acs.iecr.8b05230

Meille, V. (2006). Review on methods to deposit catalysts on structured surfaces. *Applied Catalysis A: General*, *315*, 1–17. https://doi.org/10.1016/j.apcata.2006.08.031

Mettler, M. S., Mushrif, S. H., Paulsen, A. D., Javadekar, A. D., Vlachos, D. G., & Dauenhauer, P. J. (2012). Revealing pyrolysis chemistry for biofuels production: Conversion of cellulose to furans and small oxygenates. *Energy and Environmental Science*, *5*(1), 5414–5424. https://doi.org/10.1039/c1ee02743c

Mozharov, S., Nordon, A., Littlejohn, D., Wiles, C., Watts, P., Dallin, P., & Girkin, J. M. (2011). Improved method for kinetic studies in microreactors using flow manipulation and noninvasive raman spectrometry. *Journal of the American Chemical Society*, *133*(10), 3601–3608. https://doi.org/10.1021/ja1102234

Nijhuis, T. A., Beers, A. E. W., Vergunst, T., Hoek, I., Kapteijn, F., & Moulijn, J. A. (2001). Preparation of monolithic catalysts. *Catalysis Reviews - Science and Engineering*, *43*(4), 345–380. https://doi.org/10.1081/CR-120001807

Novaković, T., Radić, N., Grbić, B., Dondur, V., Mitrić, M., Randjelović, D., Stoychev, D., & Stefanov, P. (2008). The thermal stability of porous alumina/stainless steel catalyst support obtained by spray pyrolysis. *Applied Surface Science*, *255*(5 PART 2), 3049–3055.

https://doi.org/10.1016/j.apsusc.2008.08.074

Okura, K., Okanishi, T., Muroyama, H., Matsui, T., & Eguchi, K. (2016). Ammonia Decomposition over Nickel Catalysts Supported on Rare-Earth Oxides for the On-Site Generation of Hydrogen. *ChemCatChem*, *8*(18), 2988–2995. https://doi.org/10.1002/cctc.201600610

Panda, P. K., Jaleel, V. A., & Usha Devi, S. (2006). Hydrothermal synthesis of boehmite and α-alumina from Bayer's alumina trihydrate. *Journal of Materials Science*, *41*(24), 8386–8389. https://doi.org/10.1007/s10853-006-0771-7

Pattabathula, V., & Richardson, J. (2016). Introduction to Ammonia Production. *CEP Magazine*, *2*, 69–75. https://www.aiche.org/resources/publications/cep/2016/september/introduction-ammonia-production

Peela, N. R., Mubayi, A., & Kunzru, D. (2009). Washcoating of γ-alumina on stainless steel microchannels. *Catalysis Today*, *147*(SUPPL.), 17–23. https://doi.org/10.1016/j.cattod.2009.07.026

Rajabi, L., & Derakhshan, A. A. (2010). Room temperature synthesis of boehmite and crystallization of nanoparticles: Effect of concentration and ultrasound. *Science of Advanced Materials*, *2*(2), 163–172. https://doi.org/10.1166/sam.2010.1063

Rapp, B. E. (2017). Fluids. In *Microfluidics: Modelling, Mechanics and Mathematics* (pp. 243–263). https://doi.org/10.1016/B978-1-4557-3141-1.50009-5

Rebrov, E. V., De Croon, M. H. J. M., & Schouten, J. C. (2001). Design of a microstructured reactor with integrated heat-exchanger for optimum performance of a highly exothermic reaction. Catalysis Today, 69(1–4), 183–192. https://doi.org/10.1016/S0920-5861(01)00368-6

Roberge, D. M., Ducry, L., Bieler, N., Cretton, P., & Zimmermann, B. (2005). Microreactor technology: A revolution for the fine chemical and pharmaceutical industries? *Chemical Engineering and Technology*, *28*(3), 318–323. https://doi.org/10.1002/ceat.200407128

Tanimu, A., Jaenicke, S., & Alhooshani, K. (2017). Heterogeneous catalysis in continuous flow microreactors: A review of methods and applications. *Chemical Engineering Journal*, *327*, 792–821. https://doi.org/10.1016/j.cej.2017.06.161

Uman, S., Dhand, A., & Burdick, J. A. (2020). Recent advances in shear-thinning and self-healing hydrogels for biomedical applications. Journal of Applied Polymer Science, 137(25), 1–20. https://doi.org/10.1002/app.48668

Waghode, A. N., Hanspal, N. S., Shigidi, I. M. T. A., Nassehi, V., & Hellgardt, K. (2005). Computer modelling and numerical analysis of hydrodynamics and heat transfer in non-porous catalytic reactor for the decomposition of ammonia. Chemical Engineering Science, 60(21), 5862–5877. https://doi.org/10.1016/j.ces.2005.05.019

Wang, W., Padban, N., Ye, Z., Andersson, A., & Bjerle, I. (1999). Kinetics of ammonia decomposition in hot gas cleaning. Industrial and Engineering Chemistry Research, 38(11), 4175–4182. https://doi.org/10.1021/ie990337d

Watts, P., & Wiles, C. (2007). Recent advances in synthetic micro reaction technology. *Chemical Communications*, *5*, 443–467. https://doi.org/10.1039/b609428g

Wong-Hawkes, S. Y. F., Matteo, J. C., Warrington, B. H., & White, J. D. (2007). Microreactors as New Tools for Drug Discovery and Development. In P. H. Seeberger & T. Blume (Eds.), *New Avenues to Efficient Chemical Synthesis* (pp. 39–55). Springer Berlin Heidelberg.

Yahia, E. M., Fadanelli, L., Mattè, P., & Brecht, J. K. (2019). Controlled atmosphere storage. In *Postharvest Technology of Perishable Horticultural Commodities*.

https://doi.org/10.1016/B978-0-12-813276-0.00013-4

Yin, S. F., Xu, B. Q., Zhou, X. P., & Au, C. T. (2004). A mini-review on ammonia decomposition catalysts for on-site generation of hydrogen for fuel cell applications. *Applied Catalysis A: General*, *277*(1–2), 1–9. https://doi.org/10.1016/j.apcata.2004.09.020

Ying, X., Zhang, L., Xu, H., Ren, Y. L., Luo, Q., Zhu, H. W., Qu, H., & Xuan, J. (2016). Efficient Fischer-Tropsch microreactor with innovative aluminizing pretreatment on stainless steel substrate for Co/Al 2 O 3 catalyst coating. *Fuel Processing Technology*, *143*, 51–59. https://doi.org/10.1016/j.fuproc.2015.11.005

Yuzawa, H., Mori, T., Itoh, H., & Yoshida, H. (2012). Reaction mechanism of ammonia decomposition to nitrogen and hydrogen over metal loaded titanium oxide photocatalyst. Journal of Physical Chemistry C, 116(6), 4126–4136. https://doi.org/10.1021/jp209795t

Appendices

Appendix A - Determination of HCl Volume Per Drop

We polymerized boehmite using a bottle dropper for *Initial Control* and a Pasteur pipette for our *Determination of Acid Threshold* experiment. To determine the volume of HCl added per drop, we counted the number of drops needed to obtain 1mL of water in a graduated cylinder.

Pasteur pipette:

$$\frac{33 drops}{1\ mL} * \frac{1 mL}{1000\ uL} = \ 29\ uL\ per\ drop$$

Bottle Dropper:

$$\frac{22\ drops}{1\ mL} * \frac{1 mL}{1000\ uL} = \ 45\ uL\ per\ drop$$

Appendix B. Sample Calculation for Biot and Damkohler Numbers

To calculate the Biot and Damkohler numbers, the numbers were calculated in this order

1. Reynolds Number
2. Prandtl Number
3. Nusselt Number
4. Biot Number
5. Damkohler 1 Number
6. Damkohler 2 Number

Note: All values taken from literature were for at 450 °C

Step 1: Reynolds Number

$$Re = \frac{\rho u D}{\mu}$$

p = density ammonia (kg/m^3) = 0.2937 kg/m3
u = flow speed ammonia (m/s) = 5 cm^3/min *experimental from Cameron
5 sccm = 5e-6 m^3
5e-6 m^3/ min / (pi*(0.0002)^2) / 60 sec = 0.663 m/sec
D = diameter (m) = 0.0004 m
u = dynamic viscosity = 25.32e-6 Ns/m

Re = 3.076

Step 2: Prandtl Number

$$Pr = \frac{u C_p}{k}$$

u = dynamic viscosity = 25.32e-6 N s/m^2

Cp = specific heat of ammonia = 2930 J/kgK

k = thermal conductivity of ammonia = 0.7822 W/mK

Pr = 0.948

Step 3: Nusselt Number

Nusslet Number depends on the values of Re and Pr – we are using an equation for Nu that applies to flow through cylinders from Cario University:

$$Nu = c * Re^{m} * Pr^{1/3}$$

Re_D	c	m
0.4-4	0.989	0.33
4-40	0.911	0.385
40-4000	0.683	0.466
4000-40,000	0.193	0.618
40,000-400,000	0.027	0.805

Because Re was between 0.4 and 4, coefficients for c and m were 0.989 and 0.33 respectively.

Nu = 1.408

We then used the more generalized version of the Nusselt number to determine the heat transfer coefficient of the ammonia gas through the reactor at 450 °C

$$Nu = \frac{hD}{k}$$

h = 275.3 W/m^{2}K

Step 4: Biot Number

$$Bi = \frac{h * L}{k}$$

k = thermal conductivity of the alumina and stainless steel = 14.4 W/mK
L= thickness of the stainless steel tube = 0.00005 m
h = heat transfer coefficient of ammonia (calculated from Nu and Re and Pr)
Bi = (275.3)*(0.00005 m) / 14.4
Bi = 0.000956

Step 5: Calculate Damkohler Number 1

$$Da_I = \frac{\tau_{reaction}}{\tau_{conduction}} = \frac{k}{\rho * C_p * L^2 * k_{reaction}}$$

k = thermal conductivity of ammonia = 0.07822
p = density ammonia (kg/m^3) = 0.2937 kg/m^3
C_p = specific heat of ammonia = 2930 J/kg K
L = Reactor wall thickness (steel thickness) = 50 microns

$K_{reaction\ constant}$ = 1
The conversion of ammonia to hydrogen was assumed to be about 50%, taken from various literature, specifically from (Wang et al, 1999). We then assumed the Arrhenius equation for the ammonia decomposition reaction at 450 C was comparable to k = x / (1-x) where x is the conversion of ammonia. Our k constant was then 1. Depending on the temperature of the reaction, the k value would increase.

Da_I = 0.000366

Step 6: Calculate Damkohler Number 2

$$Da_{II} = \frac{\tau_{reaction}}{\tau_{convection}} = \frac{h}{\rho * C_p * L * k_{reaction}}$$

h = heat transfer between the ammonia gas and the reactor walls
L = Reactor wall thickness (steel thickness) = 50 microns
p = density ammonia (kg/m^3) = 0.2937 kg/m^3
C_p = specific heat of ammonia = 2930 J/kg K
p = density ammonia (kg/m^3) = 0.2937 kg/m^3

To calculate the heat transfer between the ammonia gas and the reactor walls, we used the thermal sum of resistances through metal
$1/R_{tot} = 1/h_{ammonia} + L/k_{stainless\ steel} + 1/h_{air}$

$h_{ammonia}$ = 275.33 (calculated from Nu previously

$k_{stainless\ steel}$ = 14.4 W/m^{2}K

h_{air} = 50 W/m^{2}K

R_{tot} = h = 42.37 W/K

Da_{II} = 0.0399